Intramolecular hydrogen-bonding in 2-nitroresorcinol. A combined FT-IR, FT-Raman and computational study

ARTICLE *in* CHEMICAL PHYSICS · MARCH 2000

Impact Factor: 1.65 · DOI: 10.1016/S0301-0104(99)00390-0

3 AUTHORS, INCLUDING:

Gábor Keresztury
Hungarian Academy of Sciences
112 PUBLICATIONS **2,116** CITATIONS

ELSEVIER

Chemical Physics 253 (2000) 193–204

Chemical Physics

www.elsevier.nl/locate/chemphys

Intramolecular hydrogen-bonding in 2-nitroresorcinol. A combined FT-IR, FT-Raman and computational study

A. Kovács [a,*], G. Keresztury [b], V. Izvekov [a]

[a] *Research Group for Technical Analytical Chemistry of the Hungarian Academy of Sciences at the Institute of General and Analytical Chemistry, Technical University of Budapest, H-1521 Budapest, Szt. Gellért tér 4, Hungary*

[b] *Institute of Chemistry, Chemical Research Center, Hungarian Academy of Sciences, H-1525 Budapest, P.O. Box 17, Hungary*

Received 9 July 1999

Abstract

The vibrational properties of 2-nitroresorcinol have been studied by a combined experimental and theoretical analysis. The FT-IR and FT-Raman spectra of the compound have been recorded in the mid- and far-IR range (4000–150 cm^{-1}). Symmetry related experimental information was obtained from polarisation IR and Raman measurements. The interpretation of the spectra was aided by quantum chemical calculations carried out at the B3-LYP/6-31G* level. Both the spectra and calculations support the C_{2v} structure of the molecule with a symmetric intramolecular –O–H···O–N–O···H–O– hydrogen bonding interaction. The deficiencies of the computations for the molecular vibrations were corrected by the scaled quantum mechanical (SQM) method of Pulay. Using the standard scale factors developed for B3-LYP/6-31G* force fields, an rms deviation of 9.7 cm^{-1} was achieved between the gas-phase experimental and SQM frequencies. As a result of our SQM analysis, all the 42 fundamentals of the molecule were assigned. A comparison with the analogous hydrogen bonding moiety in 2-nitrophenol indicates a somewhat stronger hydrogen bonding interaction in the title molecule. This is accompanied, however, by an increased strain in the six-membered –C–O–H···O–N–C– rings.

Keywords: Hydrogen bonding; 2-Nitroresorcinol; FT-IR; FT-Raman; Scaled quantum mechanical analysis

1. Introduction

Hydrogen bonding appears in a great variety of situations, being responsible, among others, for conformational properties, for molecular packing in crystal structures, as well as for biological activity in many physiologically important systems [1,2]. We have been interested in probing into the vibrational characteristics of intramolecular hydrogen-bonded systems using vibrational spectroscopy. Our previous studies have included the investigation of 2,6-difluorophenol [3], 2-nitrophenol [4] and 2,5-dihydroxy-1,4-benzoquinone [5]. The vibrational analysis of the above molecules was based on a combination of experimental (FT-IR, FT-Raman) and theoretical information. The theoretical data were obtained by quantum chemical calculations using the Becke3-Lee–Yang–Parr (B3-LYP) method of the density functional theory (DFT) in conjunction with a 6-31G* basis set.

The DFT computations provide vibrational frequencies usually in fair agreement with experiment, however, for a reliable vibrational analysis

* Corresponding author. Tel.: +36-1-463-3414; fax: +36-1-463-3408.

E-mail address: attila.aak@chem.bme.hu (A. Kovács).

0301-0104/00/$ - see front matter
PII: S0301-0104(99)00390-0

scaling of the computed harmonic force field is required. In our previous studies, we used the selective scaling (scaled quantum mechanical, SQM) method of Pulay [6] adapted recently for B3-LYP/6-31G* force fields [7–11]. We found a good performance of the SQM method for 2-nitrophenol [4] implying that a vibrational analysis can be carried out successfully on the present derivative, on 2-nitroresorcinol (**1**) as well.

Like 2-nitrophenol, **1** contains strong intramolecular H···O hydrogen bonding, both oxygens of the nitro group interacting with the adjacent OH hydrogens in a symmetrical way (–O–H···O–N–O···H–O–) in the global minimum structure. This interaction has been investigated in various experimental and theoretical studies [12–19]. Despite the extensive investigations, however, the vibrational description of **1** is incomplete. Most spectroscopic studies [13–15] focused on the OH stretching vibrations, while Dell et al. [12] published only the band positions in the 500–1800 cm^{-1} range without any assignment. In addition, no Raman data are available for the compound, though the A_2 modes are Raman active only.

In the present article, we report our results on the vibrational characteristics of **1**. We recorded the FT-IR and FT-Raman spectra of the CCl_4 solution and solid as well as the FT-IR spectra of the gas. Based on these experimental data, a complete vibrational analysis of the molecule was performed using Pulay's DFT-based SQM method [7]. The assignment of fundamental bands to various symmetry species was supported by polarisation IR and Raman measurements.

2. Experimental

A commercial sample of 2-nitroresorcinol (Aldrich, 99% purity) was used for recording the spectra after a purity check by liquid chromatography. Gaseous, solution and solid-phase infrared spectra were recorded on a Perkin–Elmer System 2000 Fourier-transform IR spectrometer equipped with a mercury cadmium telluride (MCT) detector for the mid-IR range and with a deuterated triglycine sulphate (DTGS) detector for the far-IR range. The vapour spectra were obtained at ~75°C using a temperature controlled 10 cm gas cell (Graseby Specac). The liquid-phase spectra were recorded using 0.1 M CCl_4 solution [1] in a 0.3 and 2.0 mm liquid cell for the 4000–450 and 450–30 cm^{-1} ranges, respectively. The spectra of the solid were measured using KBr (mid-IR) and polyethylene (far-IR) pellets. With the solid and solution samples, 16 (mid-IR) and 128 scans (far-IR) were co-added, respectively, while in the gas-phase measurements 1024 scans were accumulated. The spectra of the solid and solution samples were recorded at a resolution of 4 cm^{-1}, whereas those of the vapour were recorded at 0.5 cm^{-1}.

Polarised IR spectra were measured on a Nicolet Magna 750 FT-IR spectrometer at a 2 cm^{-1} resolution with the sample aligned in uniaxially oriented nematic liquid crystal (LC). A Perkin–Elmer Au/AgCl wire grid polariser placed in front of the sample was used to produce linearly polarised radiation. The sample consisted of a 5% (m/m) solution of **1** in liquid crystal ZLI-1695 (Merck) filled into a 0.024 mm KBr liquid cell with specially pretreated windows [20]. The two absorbance spectra recorded with the electric vector of light oriented parallel and perpendicular to the director of the LC were used in a stepwise reduction process [21] to obtain the so-called reduced spectra and the dichroic ratios d_i of the IR bands by successive interactive subtractions. The orientation factors were calculated for each band from the observed dichroic ratios using the formulas given by Michl and Thulstrup [21].

The Raman spectra were measured in the 4000–150 cm^{-1} range with a Nicolet Model 950 FT-Raman spectrometer at 2 cm^{-1} resolution using the 1064 nm line of a Nd:YAG laser for excitation (at a 100–600 mW output power) and 180° scattering geometry. In general, 512 scans were co-added. Depolarisation measurements were performed on the liquid (CCl_4 solution) samples with the same set-up using a built-in polarisation analyser set parallel and perpendicular to the electric vector of the exciting laser beam. The solvent spectra were subtracted from those of the

[1] The character of the spectra did not change upon further dilution.

solution measured under the same conditions. The Raman spectra communicated here are not corrected for instrument response.

3. Computational details

Calculations were carried out using the 1993 version (G92-DFT) of the GAUSSIAN suite of programs [22] at the B3-LYP level [23,24] supplemented with the standard 6-31G* basis set. The Cartesian representation of the theoretical force constants has been computed at the fully optimised geometry. Calculated B3-LYP/6-31G* Raman activities were obtained using the GAUSSIAN 98 program package [25].

The nonredundant set of 42 natural internal coordinates has been automatically generated by the program INTC [26]. The Cartesian force field was transformed to internal space using the program TRA3 [27]. For the scaling scheme Pulay's standard (selective) scaling method [28] was used, in which the theoretical (unscaled) force constant matrix F has to be subjected to the congruent transformation $F' = T^{1/2}FT^{1/2}$, where F' is the scaled force constant matrix and T is the diagonal matrix containing the scale factors t_i. The atomic masses used for generation of the inverse kinetic energy matrix, G, were as follows: H, 1.0078; C, 12.011; O, 15.999; N, 14.007 (in atomic mass units). Scaling of the theoretical force field and solution of the secular equations were done with the program SCALE3 [29,30].

Definition of the natural internal coordinates of 2-nitroresorcinol is summarised in Table 1 together with the scale factors used [7]. The numbering of the atoms and definition of the valence (or 'primitive' internal) coordinates are given in Fig. 1. The quality of the SQM data was assessed by the root-mean-square deviation between the experimental

Table 1
Natural internal coordinates and scale factors for 2-nitroresorcinol

No.	Coordinate[a]	Description	Scale factor
In-plane			
1–6	$R_1, \ldots, R_6$	CC stretch	0.922
7–8	R_7, R_9	CO stretch	0.922
9	R_8	CN stretch	0.922
10–11	R_{10}, R_{11}	NO stretch	0.922
12–13	r_1, r_2	OH stretch	0.920
14–16	$r_3, \ldots, r_5$	CH stretch	0.920
17–18	$2^{-1/2}(\beta_1 - \beta_1')$, $2^{-1/2}(\beta_3 - \beta_3')$	CCO bend	0.990
19	$2^{-1/2}(\beta_2 - \beta_2')$	CCN bend	0.990
20	$2^{-1/2}(\beta_8 - \beta_8')$	CNO bend	0.990
21	$6^{-1/2}(2\alpha_7 - \beta_8 - \beta_8')$	NO_2 bend	0.990
22	$6^{-1/2}(\alpha_1 - \alpha_2 + \alpha_3 - \alpha_4 + \alpha_5 - \alpha_6)$	CCC bend	0.990
23	$12^{-1/2}$ $(2\alpha_1 - \alpha_2 + \alpha_3 + 2\alpha_4 + \alpha_5 + \alpha_6)$	CCC bend	0.990
24	$\frac{1}{2}$ $(\alpha_2 - \alpha_3 + \alpha_5 - \alpha_6)$	CCC bend	0.990
25–26	β_7, β_9	COH bend	0.876
27–29	$2^{-1/2}(\beta_4 - \beta_4')$, $2^{-1/2}(\beta_5 - \beta_5')$, $2^{-1/2}(\beta_6 - \beta_6')$	CCH bend	0.950
Out-of-plane			
30–31	γ_1, γ_3	CO wag	0.976
32	γ_2	CN wag	0.976
33	γ_7	NO_2 wag	0.976
34–36	$\gamma_4, \ldots, \gamma_6$	CH wag	0.976
37	$6^{-1/2}(-\tau_1 + \tau_2 - \tau_3 + \tau_4 - \tau_5 + \tau_6)$	CC torsion	0.935
38	$1/2(\tau_1 - \tau_3 + \tau_4 - \tau_6)$	CC torsion	0.935
39	$12^{-1/2}(-\tau_1 + 2\tau_2 - \tau_3 - \tau_4 + 2\tau_5 - \tau_6)$	CC torsion	0.935
40–41	$1/2(\tau_7 + \tau_7')$, $1/2(\tau_9 + \tau_9')$	CO torsion	0.935
42	$1/4(\tau_8 + \tau_8' + \tau_8'' + \tau_8''')$	CN torsion	0.831

[a] For definition of the 'primitive' internal coordinates see Fig. 1.

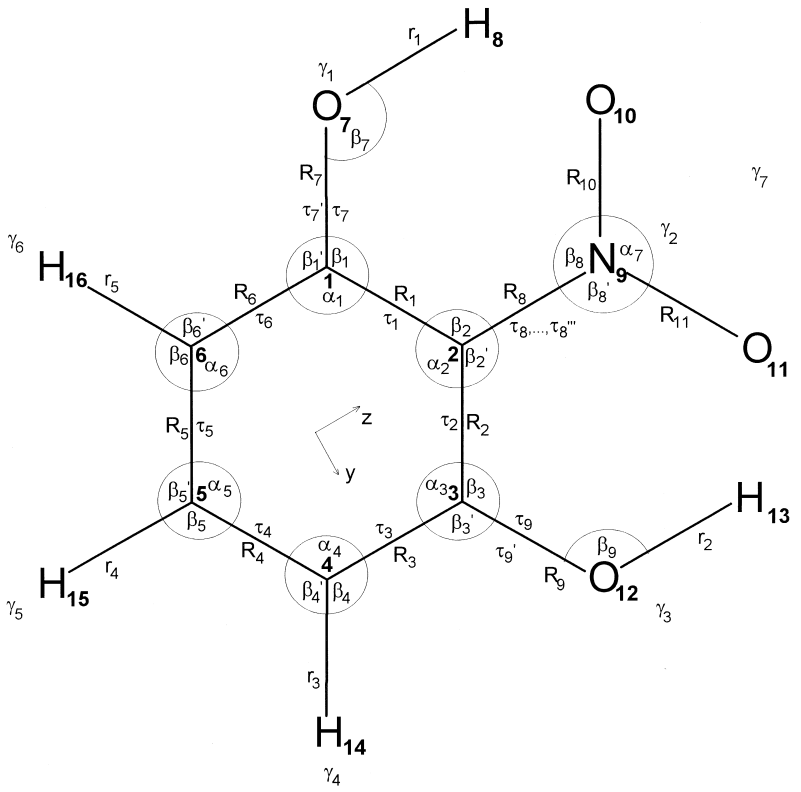

Fig. 1. Labelling of the atoms and 'primitive' valence coordinates in 2-nitroresorcin. r and R are bond stretchings, α, β and β' are in-plane valence bendings; γ and τ are wagging and torsional coordinates (defined exactly as in Ref. [42]), respectively, as follows: $\gamma_1 = \gamma_{1,7,6,2}$, $\gamma_2 = \gamma_{2,9,1,3}$, $\gamma_3 = \gamma_{3,12,2,4}$, $\gamma_4 = \gamma_{4,13,3,5}$, $\gamma_5 = \gamma_{5,14,4,6}$, $\gamma_6 = \gamma_{6,15,5,1}$, $\gamma_7 = \gamma_{9,2,11,10}$, $\tau_1 = \tau_{1,6,2,3}$, $\tau_2 = \tau_{2,1,3,4}$, $\tau_3 = \tau_{3,2,4,5}$, $\tau_4 = \tau_{4,3,5,6}$, $\tau_5 = \tau_{5,4,6,1}$, $\tau_6 = \tau_{6,5,1,2}$, $\tau_7 = \tau_{1,2,7,8}$, $\tau_7' = \tau_{1,6,7,8}$, $\tau_8 = \tau_{2,1,9,10}$, $\tau_8' = \tau_{2,1,9,11}$, $\tau_8'' = \tau_{2,3,9,10}$, $\tau_8' = \tau_{2,3,9,11}$, $\tau_9 = \tau_{2,3,12,13}$, $\tau_9' = \tau_{4,3,12,13}$.

and SQM frequencies. For characterisation of the fundamentals their total energy distribution (TED) [31,32] was used which provides a measure of each internal coordinate's contribution to the normal coordinate in terms of energy.

The unscaled force field of **1** in the natural internal coordinate representation is available from the authors upon request.

4. Results and discussion

4.1. Molecular vibrations

2-Nitroresorcinol is planar and possesses C_{2v} symmetry. Its 42 fundamentals are distributed among the symmetry species as:

$$\Gamma_{\text{vib}} = 15A_1(z) + 14B_2(y) + 5A_2 + 8B_1(x),$$

where the A_1 and B_2 fundamentals are in-plane, the A_2 and B_1 ones are out-of-plane vibrations. Only the A_1, B_1 and B_2 modes are allowed in the infrared absorption; they are accompanied by transition dipole changes along the z, x and y axes, respectively, in the molecule-fixed coordinate system (see Fig. 1). All fundamentals are active in the Raman scattering with the A_1 vibrations giving rise to polarised bands and the rest to depolarised bands.

The FT-IR and FT-Raman spectra of **1** (CCl_4 solution) are shown in Figs. 2 and 3, respectively. The results of our vibrational analysis, viz., calculated unscaled vibrational frequencies, IR intensities and Raman activities, SQM frequencies, total energy distribution (TED) and assignment of

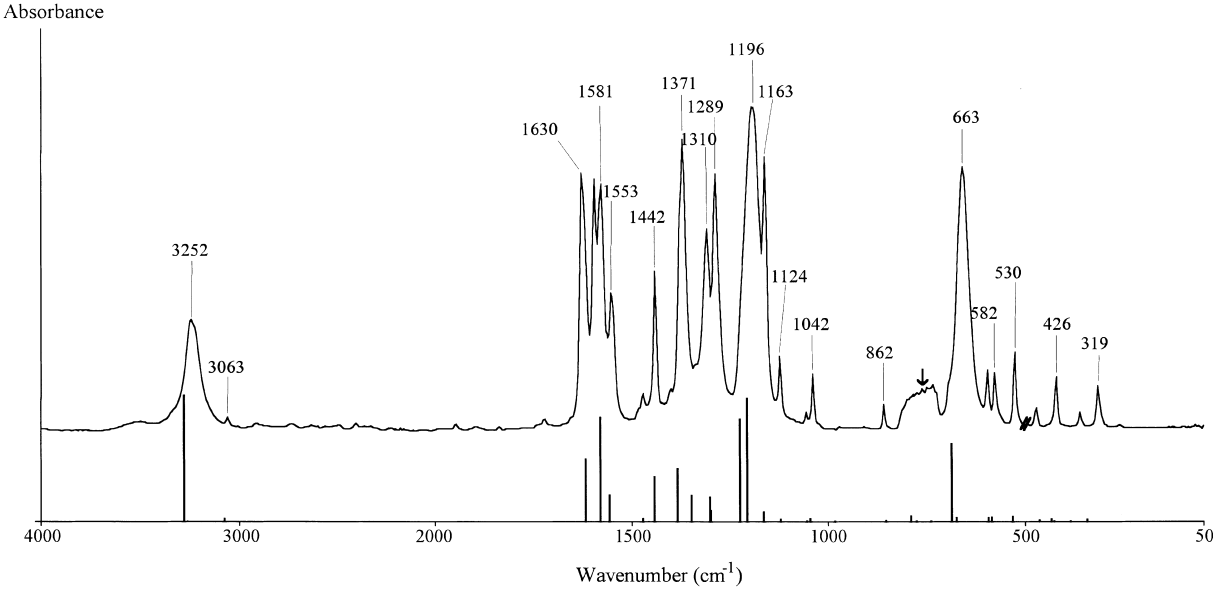

Fig. 2. Comparison of observed (top) and calculated SQM (below) IR spectra of 2-nitroresorcinol. The experimental spectrum was obtained from 0.1 M CCl_4 solution. (The arrow indicates a range of strong solvent absorption.)

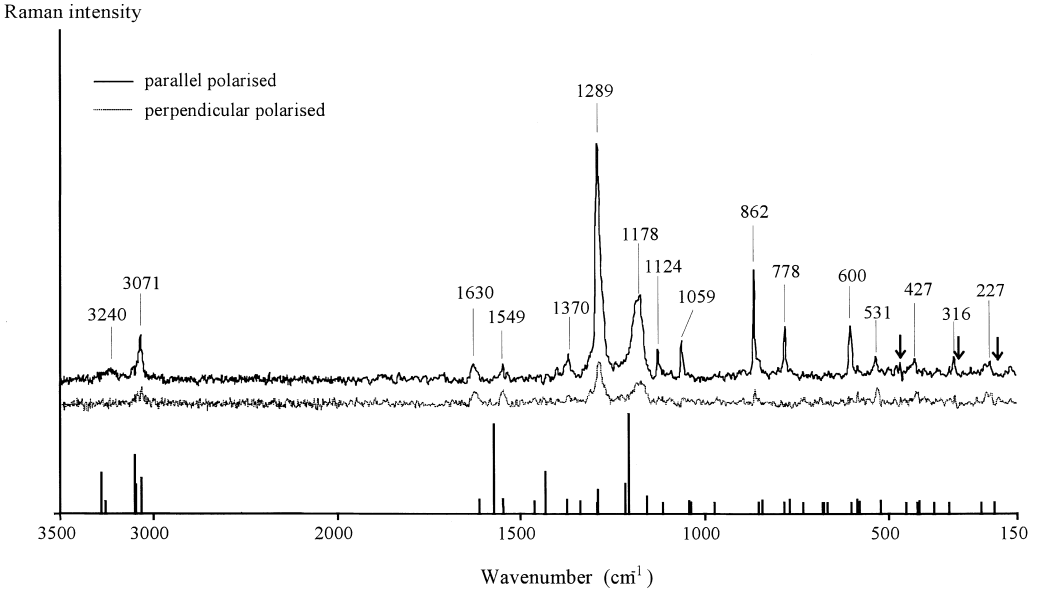

Fig. 3. Comparison of observed (top) and calculated SQM (below) Raman spectra of 2-nitroresorcinol. The experimental spectrum was obtained from 0.1 M CCl_4 solution. (The arrows indicate ranges of compensated solvent bands.)

the fundamentals, are collected in Table 2. In order to be consistent with the calculations where the isolated molecule was studied, we selected the vapour phase values of the fundamental frequencies for comparison wherever they could be located with certainty. The calculated normal modes were

Table 2
Fundamental vibrational frequencies (cm^{-1}) of 2-nitroresorcinol

	No.	Experimental[a]	Calculated[b]		Characterisation[c]
			Unscaled	Scaled	
A_1	1	3274 s	3423 (410,118)	3283	OH s (100)
	2	3114 w[d]	3237 (1,188)	3105	CH s (100)
	3	3073 vw	3204 (10,96)	3073	CH s (100)
	4	1631 s	1687 (206,16)	1624	CC s (59), COH b (10), CCC b (10)
	5	1476 vw	1541 (9,6)	1475	COH b (34), CC s (27), CCH b (27)
	6	1377 vs	1433 (173,16)	1385	CO s (40), NO s (19), CCC b (13), CC s (11)
	7	1299 s	1350 (36,62)	1299	NO s (31), COH b (19), CO s (12), CCH b (10), CC s (10)
	8	1211 vs	1279 (337,89)	1225	COH b (34), CC s (24), CN s (10), NO s (10)
	9	1121 w	1158 (7,1)	1121	CC s (28), CN s (22), CCH b (20), NO s (15), CCC b (14)
	10	1063 vw	1087 (2,9)	1053	CC s (53), CCH b (21), CCC b (14)
	11	864 vw	866 (3,12)	853	NO_2 b (43), CCC b (23), NO s (20)
	12	773 vw	792 (1,14)	778	CCC b (41), CC s (20), NO_2 b (19), CO s (13)
	13	598 vw	612 (12,15)	594	CC s (40), CN s (18), CCC b (14), NO_2 b (13), CO s (10)
	14	427 w[d]	433 (<1,8)	426	CCO b (44), CCC b (21), CC s (13), CN s (10)
	15	365 w[e]	390 (1,<1)	384	CCC b (42), CCO b (31), CN s (21)
B_2	16	3230 sh[e]	3401 (4,1)	3263	OH s (100)
	17	3085 sh[d]	3234 (2,70)	3102	CH s (100)
	18	1588 vs	1637 (342,362)	1584	CC s (53), CCC b (12), CCH b (12), NO s (10)
	19	1561 m	1625 (87,17)	1560	NO s (31), CC s (22), COH b (18), CCH b (10)
	20	1447 m	1500 (146,144)	1444	CCH b (34), CC s (23), NO s (22), COH b (11)
	21	1357 sh[f]	1412 (85,9)	1349	CC s (55), COH b (26), NO s (10)
	22	1333 m	1351 (80,1)	1301	CCH b (35), CO s (19), NO s (16), CC s (13), COH b (13)
	23	1207 vs	1268 (404,409)	1215	CC s (43), COH b (24), CO s (16), CCH b (10)
	24	1164 s	1200 (31,30)	1166	CCH b (77), CC s (19)
	25	1043 w	1081 (9,2)	1046	CO s (34), CC s (29), CCH b (12), CCN b (10)
	26	582 vw	595 (14,4)	586	CCO b (43), CNO b (28), CC s (20)
	27	530 w	535 (16,11)	530	CCC b (71), CC s (10)
	28	426 w[e]	437 (8,1)	433	CNO b (50), CCO b (38)
	29	319 m[e]	345 (7,1)	342	CCN b (78)
A_2	30	851 sh[d]	870 (–,2)	862	CH w (89), CO w (11)
	31	700 vw[g]	710 (–,1)	685	CO t (100)
	32	614 vw[g]	622 (–,1)	611	CO w (77), CC t (17)
	33	227 w[d]	225 (–,2)	218	CC t (92)
	34	60 ± 10[h]	90 (–,<1)	82	CN t (97)
B_1	35	976 w[e]	990 (<1,<1)	983	CH w (100)
	36	803 m	800 (17,2)	792	CH w (77), CO w (19)
	37	769 w[e]	748 (2,<1)	740	NO_2 w (85), CN w (15)
	38	674 s	713 (256,<1)	688	CO t (95)
	39	673 sh[e]	692 (13,1)	674	CC t (66), CO w (34)
	40	472 vw	474 (4,1)	461	CC t (75), CO w (19), CN w (14)
	41	266 w[e]	261 (1,<1)	256	CN w (52), CO w (23), CC t (20)
	42	97 vw[f]	115 (~0,1)	112	CC t (75), CN w (22)

[a] Present study, gaseous phase unless otherwise noted; vs, s, m, w, vw, sh mean very strong, strong, medium, weak, very weak and shoulder, respectively.
[b] Calculated at the B3-LYP/6-31G* level. Scaling of the harmonic force field was done by the scale factors given in Table 1. Calculated unscaled IR intensities (km mol^{-1}) and Raman activities ($Å^4$/atomic mass unit) in parentheses.
[c] For an approximate characterization of the fundamentals the total energy distribution (TED) in internal coordinates (%) is given. Only contributions greater than 10% were considered. The abbreviations s, b, w, and t mean stretch, in-plane bend, wag, and torsion, respectively.
[d] From the Raman spectrum of 0.1 M CCl_4 solution.
[e] From the IR spectrum of 0.1 M CCl_4 solution.
[f] From the IR spectrum of the solid.
[g] From the IR spectrum of the LC solution.
[h] From a microwave study [17].

primarily assigned to the observed band by closeness of their frequencies, then the correspondence of the band polarisation characteristics to the symmetry species of the modes obtained from the calculations was checked to confirm or revise the assignment. Note that we did not attempt to assign the vibrations of **1** to the normal modes of benzene (as has been customary in the past [33]), since a recent study of phenol has shown [34] that this procedure may not be justified for the in-plane vibrations of substituted benzene derivatives. Assignment of the OH group vibrations was further supported by deuteration experiments. Table 3 gives the experimental data of all the fundamentals observed in the spectra of the various (gas, solution, solid) samples.

Out of the altogether 42 fundamentals of **1**, 41 were identified in our vibrational spectra. Twenty-four fundamentals were observed in the IR spectrum of the gas, eight additional fundamentals were assigned from the IR spectrum of the CCl_4 solution, while two and three more from the IR spectrum of the solid and of the LC solution, respectively (cf. Table 3). Among the IR active A_1, B_1, and B_2 fundamentals only two (ν_2 and ν_{17}) could not be identified in our IR spectra. Their experimental frequencies, together with those of the A_2 modes were taken from the Raman spectrum of the CCl_4 solution. Only one fundamental could not be observed in our experimental spectra, viz., ν_{34} of the A_2 species which falls outside the detection range of our Raman spectrometer; for this frequency, we have an estimated value from a recent microwave study [17].

Now, a few words to assess the performance of the computed force field: the well-known reliability of density functional theory for estimation of the vibrational spectra of organic compounds can be observed also in the case of **1**. In agreement with experience [35], the unscaled B3-LYP/6-31G* vibrational frequencies are generally somewhat higher than the experimental values (cf. Table 2), their rms deviation being 78 cm^{-1}. Excluding the fundamentals above 3000 cm^{-1} from the comparison (those with the largest absolute error), the rms deviation decreases to 43 cm^{-1}. The SQM treatment improves the agreement between the experimental and scaled frequencies considerably, leading to an rms deviation of 13 cm^{-1} over all the 42 fundamentals. The present results further support the earlier found good performance of the DFT-based SQM method for N–O moieties [7,9] as well as for hydrogen bonding between the NO_2 and OH groups [4].

Large deviations (>20 cm^{-1}) between the experimental and SQM frequencies were observed for four fundamentals, ν_{16}, ν_{22}, ν_{29} and ν_{37}. The scaled force field underestimates the frequency of ν_{22} by 32 cm^{-1}, however, it gives a very good agreement for ν_{20}, a fundamental that has a similar total energy distribution. This makes the possibility of a systematic error less probable. Unfortunately, the spectral range around ν_{22} is very crowded which hinders to obtain a definite explanation (Fermi resonance or only an accidental large error of the computed force field?) for this deviation. In the case of the other three fundamentals, we have only solution data for comparison. Interaction with the solvent molecules may somewhat influence the experimental data, especially those of the polar hydroxy and nitro groups. An example of this is the 22 cm^{-1} decrease of ν_1 on changing from gas phase to CCl_4 solution (cf. Table 3), in good agreement with the deviation observed for ν_{16}.

4.2. Analysis of the IR and Raman spectra

In this section, we analyse the experimental IR and Raman data of **1** obtained from various (gaseous, liquid, solid) state samples. In general, a good agreement can be observed between the measured fundamental frequencies in the different states (cf. Table 3). The frequency scatter in the various phases is significant only for four fundamentals, ν_1, ν_7, ν_{19} and ν_{22}. These modes involve large contributions from vibrations of the hydroxy and nitro groups which are especially sensitive to intermolecular interactions in the solid phase and to solvation effects.

We note the very good agreement between the gas-phase experimental and SQM frequencies, the rms deviation being 9.7 cm^{-1}. As expected, the agreement between experiment and calculations is somewhat worse for the solution and solid-phase spectra.

Table 3
Comparison of the measured vibrational spectra[a] of 2-nitroresorcinol

Sym.	v_i	Infrared				Raman	
		Gas	CCl_4 solution	LC solution[b]	Solid	CCl_4 solution	Solid
A_1	1	3274 s	3252 s	3310 s (z)	3258 s	3240 w p	3252 vw
	2					3114 w p	3102 sh
	3	3073 vw	3063 vw	3063 vw (z)	3068 w	3071 m p	3065 m
	4	1631 s	1630 vs	1628 s (z)	1628 vs	1630 m p	1614 s
	5	1476 vw	1474 w	1466 w (z)	1477 w		1477 vw
	6	1377 vs	1371 vs	1369 s (z)	1374 s	1370 m p	1373 m
	7	1299 s	1289 s	1287 m (z)	1281 s	1289 vs p	1279 vs
	8	1211 vs	1196 vs	1170 m (z)	1195 vs	1178 s p	1204 w
	9	1121 w	1124 w	1123 w (z)	1126 w	1124 w p	1126 m
	10	1063 vw	1059 w	1058 w (z)	1059 w	1059 m p	1060 m
	11	864 vw	862 w	861 w (z)	862 w	862 s p	863 s
	12	773 vw	solv	778 vw (z)	778 w	778 m p	782 s
	13	598 vw	600 w	599 w (z)	599 w	600 m p	605 s
	14			428 vw (z)		427 w p	431 m
	15		365 w		362 w		365 vw
B_2	16		3230 sh	3218 sh (y)			
	17				3091 w	3085 sh dp	3088 m
	18	1588 vs	1581 vs	1580 s (y)	1583 vs		
		1603 vs	1598 s	1597 m (y)	1596 sh		
	19	1561 m	1553 s	1548 m (y)	1543 m	1549 vw dp	1545 s
	20	1447 m	1442 m	1438 sh (y)	1442 m		1437 w
	21			1360 m (y)	1357 sh		1362 sh
	22	1333 m	1310 s	1309 m (y)	1312 m	1308 sh dp	1316 w
	23	1207 vs	1191 vs	1194 vs (y)	1195 vs	1192 sh dp	1204 w
	24	1164 s	1163 s	1161 s (y)	1168 s	1178 s dp	1164 s
	25	1043 w	1042 w	1040 w (y)	1047 vw		1037 m
	26	582 vw	582 w	581 w (y)	579 m	581 w dp	580 m
	27	530 w	530 m	531 w (y)	535 w	531 w dp	535 m
	28		426 w	424 vw (y)	424 m		422 sh
	29		319 m		314 m	316 w dp	319 m
A_2	30			857 vw (x)		851 sh dp	851 sh
	31			700 vw (x)			
	32			614 vw (x)			
	33					227 w dp	239 m
	34						
B_1	35		976 w		991 vw		
	36	803 m		801 s (x)	809 s		809 w
	37			769 vw (x)	773 w		
	38	674 s	663 vs	668 s (x)	647 vs		
	39		673 sh				
	40	472 vw	476 w	476 vw (x)	474 w		
	41		266 w		267 vw		
	42				97 vw		

[a] The abbreviations vs, s, m, w, vw, sh mean very strong, strong, medium, weak, very weak and shoulder, respectively.
[b] Direction of transition dipole changes (x, y, z) indicated in parentheses.

In the IR spectra of the solution and solid, where the band structures are less complex due to the absence of rotational envelope, four strong bands can be observed between 1540 and 1640 cm^{-1}. The calculations, however, indicate only three fundamentals in this range, viz., v_4, v_{18}

and ν_{19}. Based on the SQM frequencies, ν_4 and ν_{19} can be unambiguously assigned to the strong bands at ~1630 and 1560 cm^{-1}, respectively. From the other two bands, the more intense one (~1580 cm^{-1}) is supposed to represent the ν_{18} fundamental. The intensity of the fourth (1597 cm^{-1}) band, however, is much greater than expected for a simple overtone or combination band. In our opinion, a Fermi resonance interaction between ν_{18} and the combination $\nu_{10} + \nu_{27}$ (1063 + 530) may be responsible for the enhanced intensity of this band. Support to the idea of Fermi resonance is provided by the polarised IR spectra, indicating that both the 1580 and 1597 cm^{-1} bands (and additionally, the 1560 cm^{-1} band) belong to the same symmetry species (B_2). Another Fermi resonance interaction is encountered between ν_8 and $2\nu_{26}$ (2×582) near 1160 cm^{-1} which is best seen in the LC solution spectra.

In order to get some theoretical information on the Raman activity of the fundamentals, we performed calculations at the B3-LYP/6-31G* level using the recently available 'Raman' option in the GAUSSIAN 98 program [25]. The experimental and theoretical Raman spectra are presented in Fig. 3. The comparison shows great errors of the computed Raman activities. Most striking are the computed very large activities of the ν_1, ν_{18}, ν_{20} and ν_{23} fundamentals, while the experimental spectrum shows only weak scattering activities for these modes. In view of these deficiencies of the theoretical data, we neglected them at the interpretation of the experimental Raman spectra.

The good solubility of **1** in CCl_4 allowed us to perform Raman depolarisation experiments, where the detection of polarized bands was used to support the assignment of the A_1 fundamentals. Note that the back-scattering geometry and large collection angle of our FT-Raman spectrometer are not ideally suited to precise depolarisation measurements; thus, the measured data can only be indicative. Hence, some surely depolarised bands (e.g. ν_{27} at 531 cm^{-1}) have ρ values close to 1.0 instead of the theoretically predicted 0.75 (cf. Fig. 3), and the polarised bands may also have ρ values higher than the expected theoretical ones.

4.3. Linear dichroism and symmetry of molecular dynamics

The analysis of the two polarized IR absorbance spectra ($A_\parallel$ and $A_\perp$) has shown that each absorption band of **1** possesses one of three well distinguishable dichroic ratio values ($d = A_\parallel/A_\perp$) $d_x = 0.386$, $d_y = 1.044$, and $d_z = 1.81$. These values, in turn, lead to three different orientation factors: $K_x = 0.16$, $K_y = 0.34$, and $K_z = 0.48$, the sum of which comes close to unity. This means that the vibrational transition moments are aligned along three mutually perpendicular directions, with K_z corresponding to the direction of the longest and K_x to the shortest dimension of the molecule. Thus, the linear dichroism measurements confirm the very nearly planar structure of the molecule in LC solution, with C_{2v} effective symmetry. The dichroic ratio values can be used as firm indicators to assign the observed bands to the corresponding IR active symmetry species, as is done in the appropriate column of Table 3 (indicated as x, y, and z in parentheses).

The above-mentioned dichroic ratio values served as subtraction factors to obtain the three so-called *reduced* linear dichroism spectra (see Fig. 4) that emphasize the difference in dichroic behavior of the bands [21]. In these spectra, bands belonging to one of the three IR active symmetry species are eliminated. For example, the x-reduced spectrum, Δ_{yz}, in which the x-polarized out-of-plane bands are missing (top trace in Fig. 4), is obtained by $\Delta_{yz} = A_\parallel - d_x A_\perp$. Note that the band of CO torsion (the strong, broad feature at 668 cm^{-1}) is eliminated together with the CH wagging bands (e.g., 801 cm^{-1}), proving that the OH bonds are within the plane of the benzene ring at equilibrium.

An interesting phenomenon in the LC solution spectra is that some of the principally IR-inactive transitions belonging to the A_2 species show up as very weak absorption features, with out-of-plane polarization. This may be due to slight deviations from the average C_{2v} symmetry in a statistically significant number of molecules due to solvent–solute interactions.

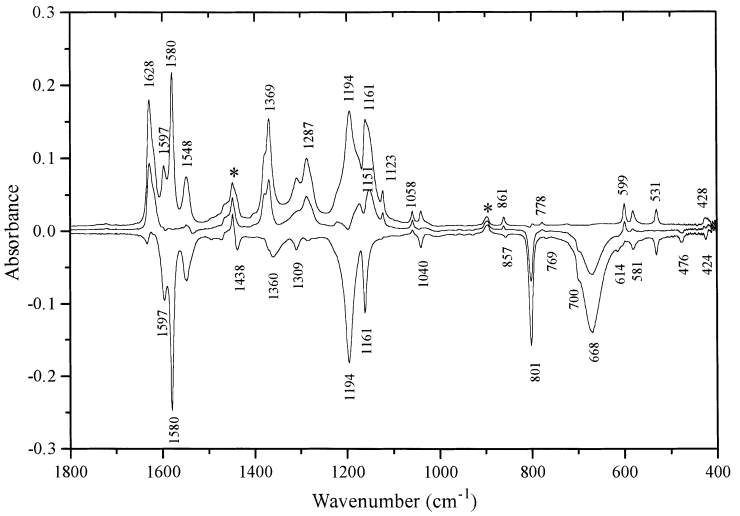

Fig. 4. Reduced linear dichroism IR spectra of 2-nitroresorcinol in the 1800–400 cm^{-1} region: Δ_{yz} (top), Δ_{xz} (middle), and Δ_{xy} (lower trace); asterisks indicate uncompensated absorption of LC solvent.

4.4. Intramolecular hydrogen bonding

The –O–H···O–N– interaction in **1** is very similar in its characteristics to the analogous interaction in 2-nitrophenol. An interesting question is the effect of the second hydroxy group (forming a second hydrogen bond) on the strength of the original hydrogen bonding. In Table 4, we compiled the geometrical and vibrational characteristics of this interaction found in the two molecules.

The strength of the interaction can be related to the length of the hydrogen bond. The gas electron diffraction technique is able to determine the position of hydrogen atoms only with large uncertainty. This is reflected in the O···H distances given in Table 4, where the values of the two molecules agree within (the large) experimental error. Calculations at the B3-LYP/6-31G* level indicate a shorter (by 0.02 Å) hydrogen bond in 2-nitroresorcinol in agreement with both the calculated and experimental nonbonded O···N distances. Hence, the closer position of the interacting H and O in **1** refers to a somewhat stronger interaction in that molecule as compared to 2-nitrophenol. On the other hand, the vibrational data indicate that the doubly hydrogen bonded system contains more strain than the single six-membered –C–O–H···O–N–C– ring in 2-nitrophenol. Both the decrease of the OH stretching frequency (associated with the lengthening of the O–H bond) and the increase of the CO and NO torsional frequencies upon hydrogen bonding (associated with the constraining effect of the hydrogen bond) are somewhat higher in 2-nitrophenol.

The other vibrations of these groups are not informative in this respect because, as usual, they are strongly mixed with each other and with the vibrations of the phenyl ring (cf. Table 2). Except for the CCN bend (ν_{29}), the largest contributions of the other OH and NO_2 in-plane vibrations are around 45% in the fundamentals (e.g. 50% CNO bend in ν_{28}, 44% and 43% CCO bend in ν_{14} and ν_{26}, respectively, 43% NO_2 bend in ν_{11}). The NO stretchings dominate in ν_7 and ν_{19}, but with a rather low (31%) contribution. The CO stretch has a substantial contribution in three (ν_6, ν_7, ν_{25}), the COH bend in six (ν_5, ν_8, ν_{19}, ν_{21}, ν_{22}, ν_{23}) and the CCO in-plane bend in four (ν_{14}, ν_{15}, ν_{26}, ν_{28}) fundamentals. The CN stretch appears as minor contribution only (in ν_9, ν_{13}, and ν_{15}). In contrast to 2-nitrophenol [4], the CO wag, NO_2 wag and CN wag motions appear as major contribution in the fundamentals ν_{32}, ν_{37} and ν_{41}, respectively.

Most of the phenyl ring modes involve only minor contributions from vibrations of the OH and NO_2 moieties, hence these modes are not

Table 4
Geometrical and vibrational characteristics of the –O–H···O–N– intramolecular hydrogen bonding interaction in 2-nitrophenol and 2-nitroresorcinol (**1**)

Parameter	Method	2-nitrophenol	2-nitroresorcinol
O···H (Å)	electron diffraction	1.72(2)[a]	1.76(4)[b]
	B3-LYP/6-31G*	1.712[c]	1.691
O···N (Å)	electron diffraction	2.58(1)[a]	2.56(1)[b]
	B3-LYP/6-31G*	2.578[c]	2.556
$\Delta\nu_{OH}$ (cm^{-1})[d]	IR	−402	−380
$\Delta\tau_{CO}$ (cm^{-1})[e]	IR	+380	+346
$\Delta\tau_{CN}$ (cm^{-1})[f]	IR, MW	ca. + 35	ca. + 10

[a] From Ref. [36].
[b] From Ref. [16].
[c] From Ref. [4].
[d] Change of the OH stretching frequency of the title molecules with respect to that of the parent phenol [34] and resorcinol [37], respectively. The frequencies were taken from gas-phase IR measurements, that of 2-nitrophenol from Ref. [4].
[e] Change of the CO torsional frequency of the title molecules with respect to that of the parent phenol and resorcinol, respectively. The frequencies were taken from gas-phase IR measurements for phenol [38] and 2-nitrophenol [4], while from the IR spectrum of cyclohexane solution for resorcinol [39] and **1**.
[f] Change of the CN torsional frequency of the title molecules with respect to that of the parent nitrobenzene. The frequencies were obtained from microwave data for nitrobenzene [40] and **1** [17] and from the IR spectrum of octane solution for 2-nitrophenol [41].

particularly sensitive to the hydrogen bonding interaction and to the effects of the surroundings in the solution and solid. This latter feature is reflected in the small variation of these fundamental frequencies in the gas and solution phases (Table 3).

5. Conclusions

Presently, the DFT-based SQM approach provides the most reliable theoretical information on the vibrational properties of medium-size molecules. This method, using Pulay's standard scale factors, performed well for 2-nitroresorcinol. Based on the SQM force field, a complete vibrational analysis of the title compound was performed resulting in the assignment of all the 42 fundamentals of **1**. The overall good quality of the SQM force field is characterised by the achieved root mean square deviation of 9.7 cm^{-1} between the gas-phase experimental and SQM frequencies. The assignment of most of the fundamentals suggested in the present study is unambiguous, having taken advantage of polarisation IR and Raman experimental data as well as the effective scaling and the fairly good IR intensity information from DFT.

Introduction of a second intramolecular hydrogen bonding at the other side of the nitro group has little effect on the –O–H···O–N– hydrogen bonding interaction. The decreased hydrogen bond length is in agreement with a marginal strengthening of the original interaction accompanied by a (marginally) increased strain inside of the six-membered –C–O–H···O–N–C– ring as indicated by the vibrational data.

Acknowledgements

This work has been supported by the Hungarian Scientific Research Foundation (OTKA No. T030053).

References

[1] G.C. Pimentel, A.L. McClellan, The Hydrogen Bond, Freeman, San Francisco, 1960.
[2] G.A. Jeffrey, W. Saenger, Hydrogen Bonding in Biological Structures, Springer, Berlin, 1991.
[3] I. Macsári, V. Izvekov, A. Kovács, Chem. Phys. Lett. 269 (1997) 393.
[4] A. Kovács, V. Izvekov, G. Keresztury, G. Pongor, Chem. Phys. 238 (1998) 231.
[5] A. Szabó, A. Kovács, J. Mol. Struct. 510 (1999) 215.

[6] P. Pulay, G. Fogarasi, G. Pongor, J.E. Boggs, A. Vargha, J. Am. Chem. Soc. 105 (1983) 7037.
[7] G. Rauhut, P. Pulay, J. Phys. Chem. 99 (1995) 3093.
[8] P.M. Kozlowski, G. Rauhut, P. Pulay, J. Chem. Phys. 103 (1995) 5650.
[9] A. Kovács, K.B. Borisenko, G. Pongor, Chem. Phys. Lett. 280 (1997) 451.
[10] A. Kovács, V. Izvekov, J. Mol. Struct. 410–411 (1997) 403.
[11] P.M. Kozlowski, A.A. Jarzecki, P. Pulay, J. Phys. Chem. 100 (1996) 7007.
[12] H.-D. Dell, R. Kamp, M. Doersing, H. Jansen, Liebigs Ann. Chem. 709 (1967) 70.
[13] V.A. Granzhan, L.M. Savenko, S.V. Semenenko, S.K. Laktionova, Zh. Strukt. Khim. 12 (1971) 809.
[14] E.E. Milliaresi, V.E. Rutskin, Dokl. Akad. Nauk SSSR 198 (1971) 108.
[15] P.G. Hall, G.S. Horsfall, J. Chem. Soc. Faraday Trans. 2 (69) (1973) 1078.
[16] K.B. Borisenko, I. Hargittai, J. Phys. Chem. 97 (1993) 4080.
[17] W. Caminati, B. Velino, R. Danieli, J. Mol. Spectrosc. 161 (1993) 208.
[18] C.W. Bock, I. Hargittai, Struct. Chem. 5 (1994) 307.
[19] G. Chung, O. Kwon, Y. Kwon, J. Phys. Chem. A 101 (1997) 4628.
[20] M. Belhakem, B. Jordanov, J. Mol. Struct. 218 (1990) 309.
[21] J. Michl, E.W. Thulstrup, Spectroscopy with Polarized Light: Solute Alignment by Photoselection, in Liquid Crystals, Polymers, and Membranes, VCH, New York (Chapter 5), 1986, pp. 222–268.
[22] M.J. Frisch, G.W. Trucks, M. Head-Gordon, P.M.W. Gill, M.W. Wong, J.B. Foresman, B.G. Johnson, H.B. Schlegel, M.A. Robb, E.S. Replogle, R. Gomperts, J.L. Andres, K. Raghavachari, J.S. Binkley, C. Gonzalez, R.L. Martin, D.J. Fox, D.J. DeFrees, J. Baker, J.J.P. Stewart, J.A. Pople, GAUSSIAN 92/DFT, Revision F, Gaussian, Pittsburgh, 1993.
[23] A.D. Becke, J. Chem. Phys. 98 (1993) 5648.
[24] C. Lee, W. Yang, R.G. Parr, Phys. Rev. B 37 (1988) 785.
[25] M.J. Frisch, G.W. Trucks, H.B. Schlegel, G.E. Scuseria, M.A. Robb, J.R. Cheeseman, V.G. Zakrzewski, J.A. Montgomery Jr., R.E. Stratmann, J.C. Burant, S. Dapprich, J.M. Millam, A.D. Daniels, K.N. Kudin, M.C. Strain, O. Farkas, J. Tomasi, V. Barone, M. Cossi, R. Cammi, B. Mennucci, C. Pomelli, C. Adamo, S. Clifford, J. Ochterski, G.A. Petersson, P.Y. Ayala, Q. Cui, K. Morokuma, D.K. Malick, A.D. Rabuck, K. Raghavachari, J.B. Foresman, J. Cioslowski, J.V. Ortiz, B.B. Stefanov, G. Liu, A. Liashenko, P. Piskorz, I. Komaromi, R. Gomperts, R.L. Martin, D.J. Fox, T. Keith, M.A. Al-Laham, C.Y. Peng, A. Nanayakkara, C. Gonzalez, M. Challacombe, P.M.W. Gill, B. Johnson, W. Chen, M.W. Wong, J.L. Andres, C. Gonzalez, M. Head-Gordon, E.S. Replogle, and J.A. Pople, GAUSSIAN 98, Revision A.5, Gaussian, Inc., Pittsburgh PA, 1998.
[26] G. Fogarasi, X. Zhou, P.W. Taylor, P. Pulay, J. Am. Chem. Soc. 114 (1992) 8191.
[27] J.M. Coffin, P. Pulay, Program TRA3, Dept. of Chemistry and Biochemistry, University of Arkansas, Fayetteville, AR, 1989.
[28] P. Pulay, Applications of electronic structure theory, in: H.F. Schaefer III (Ed.), Modern Theoretical Chemistry, vol. 4, Plenum, New York, 1977, p. 153.
[29] G. Pongor, G. Fogarasi, I. Magdó, J.E. Boggs, G. Keresztury, I.S. Ignatyev, Spectrochim. Acta 48A (1992) 111.
[30] G. Pongor, Program SCALE3, Dept. of Theoretical Chemistry, Eötvös Loránd University, Budapest, Hungary, 1993.
[31] P. Pulay, F. Török, Acta Chim. Hung. 44 (1965) 287.
[32] G. Keresztury, G. Jalsovszky, J. Mol. Struct. 10 (1971) 304.
[33] G. Varsányi, Assignment for Vibrational Spectra of 700 Benzene Derivatives, Hilger, London, 1974.
[34] G. Keresztury, F. Billes, M. Kubinyi, T. Sundius, J. Phys. Chem. A 102 (1998) 1371.
[35] A.P. Scott, L. Radom, J. Phys. Chem. 100 (1996) 16502.
[36] K.B. Borisenko, C.W. Bock, I. Hargittai, J. Phys. Chem. 98 (1994) 1442.
[37] H.W. Wilson, Spectrochim. Acta 30A (1974) 2141.
[38] M. Kubinyi, F. Billes, A. Grofcsik, G. Keresztury, J. Mol. Struct. 266 (1992) 339.
[39] W.G. Fateley, G.L. Carlson, F.F. Bentley, J. Phys. Chem. 79 (1975) 199.
[40] J.H. Høg, L. Nygaard, G.O. Sørensen, J. Mol. Struct. 7 (1971) 111.
[41] V.M. Schreiber, J. Mol. Struct. 197 (1989) 73.
[42] S. Califano, Vibrational States, Wiley, London, 1976, pp. 84–87.